The EMBO Journal (2005) 24, 1397–1405 | © 2005 European Molecular Biology Organization | All Rights Reserved 0261-4189/05
www.embojournal.org

THE EMBO JOURNAL

Biglycan is a new extracellular component of the Chordin–BMP4 signaling pathway

Mauricio Moreno, Rosana Muñoz, Francisco Aroca, Mariana Labarca, Enrique Brandan and Juan Larraín*

Department of Cell and Molecular Biology, Centre for Cell Regulation and Pathology, Millennium Nucleus in Developmental Biology, Faculty of Biological Sciences, P. Universidad Católica de Chile, Alameda, Santiago, Chile

The BMP4 signaling pathway plays key roles during early embryonic development and for maintenance of adult homeostasis. In the extracellular space, BMP4 activity is regulated by a group of interacting molecules including the BMP antagonist Chordin, the metalloproteinase Tolloid and Twisted gastrulation (Tsg). In this study, we identified Biglycan (Bgn), a member of the small leucine-rich proteoglycan family, as a new extracellular modulator of BMP4 signaling. *Xenopus* Bgn (*xBgn*) is expressed uniformly in the ectoderm and mesoderm and their derivatives during development. Microinjection of *Bgn* mRNA induced secondary axes, dorsalized the mesoderm and inhibited BMP4 activity in *Xenopus* embryos. Biochemical experiments showed that Bgn binds BMP4 and Chordin, interaction that increased binding of BMP4 to Chordin. Bgn was also able to improve the efficiency of Chordin–Tsg complexes to block BMP4 activity. Using antisense morpholinos, we demonstrated that Bgn required Chordin to induce double axes in *Xenopus*. This work unveiled a new function for Bgn, its ability to regulate BMP4 signaling through modulation of Chordin anti-BMP4 activity.

The EMBO Journal (2005) **24,** 1397–1405. doi:10.1038/sj.emboj.7600615; Published online 17 March 2005
Subject Categories: signal transduction; development
Keywords: Biglycan; BMP signaling; Chordin; embryonic patterning; extracellular matrix

Introduction

Embryonic patterning is established by morphogenetic gradients during early development. Dorsoventral patterning of vertebrate and invertebrate embryos has been well studied and is one of the paradigms for understanding morphogen function (Freeman and Gurdon, 2002). An extracellular gradient of BMP4 activity determines cell-fate decisions along the dorsoventral axis. This extracellular gradient is generated during gastrulation by an array of secreted proteins including Chordin (Chd), Xolloid (Xld) and Twisted gastrulation (Tsg; De Robertis *et al*, 2000). Chd is the central regulator of BMP4 activity; it binds BMP4 through conserved cysteine-rich domains (CRs) and blocks binding of the growth factor to its cognate receptor (Piccolo *et al*, 1996, Larraín *et al*, 2000). The levels of Chd anti-BMP activity are finely regulated by Tsg and Xld. Tsg binds BMP4 and Chd making a ternary complex that tightly sequesters BMP4 (Oelgeschläger *et al*, 2000). This complex is inactivated by the metalloproteinase Xld, which cleaves Chd releasing BMP4, Chd fragments and Tsg (Larraín *et al*, 2001). More recently, Tsukushi, a chondroitin sulfate proteoglycan (CSPG), has been shown to function in this molecular pathway (Ohta *et al*, 2004). It has been proposed that this biochemical reaction produces the right levels of BMP4 activity along the dorsoventral axis allowing proper patterning (De Robertis *et al*, 2000).

Proteoglycans (PGs) are abundant extracellular molecules that consist of a core protein to which different highly sulfated glycosaminoglycan (GAG) chains are attached. Depending on the sugar content, the GAG chains could be of heparan sulfate (HS), chondroitin sulfate (CS) or dermatan sulfate (DS) (Iozzo, 1998; Bernfield *et al*, 1999). PGs could be classified into several families based on their core protein structure. Glypicans and Syndecans are two major cell surface heparan sulfate proteoglycans (HSPGs) and Perlecans are mainly distributed in the extracellular matrix (Bernfield *et al*, 1999). Members of the small leucine-rich proteoglycan (SLRP) family are the most studied among CSPGs. These are secreted PGs with a central domain containing leucine-rich repeats (LRRs) flanked at either side by small cysteine clusters. Decorin (Dcn) and Biglycan (Bgn) are the prototype members of this family (Iozzo, 1998) and Tsukushi is a recently described member of this family (Ohta *et al*, 2004). Biochemical and cell culture assays have implicated PGs as coregulators of many growth factors such as FGF, HGF, Wnt, TGF-β, BMP, etc. (Iozzo, 1998; Bernfield *et al*, 1999). The importance of HSPGs during early embryonic development of invertebrate and vertebrate embryos has been clearly established by genetic studies (Perrimon and Bernfield, 2000). *In vitro* analysis showed that HSPGs play crucial roles in regulating key developmental signaling pathways, such as the Wnt, Hedgehog, TGF-β and FGF pathways. In these studies, mutations in the enzymes responsible for the biosynthesis of GAG chains have unveiled the importance of all PGs in development. Even though this approach has been fundamental for our understanding of PG function, it does not help to address the role of specific PGs. To study the role of specific PGs during development, we decided to identify biochemically the PGs synthesized during early development of the *Xenopus* embryo and then to analyze its function.

As shown here, we have identified *Xenopus* Bgn (*xBgn*), which is expressed early during development. Microinjection of *Bgn* mRNA induced secondary axes, dorsalized the mesoderm and inhibited BMP4 activity in *Xenopus* embryos. Biochemical experiments showed that Bgn binds BMP4 and

*Corresponding author. Department of Cell and Molecular Biology, Centre for Cell Regulation and Pathology, Millennium Nucleus in Developmental Biology, Faculty of Biological Sciences, P. Universidad Católica de Chile, Alameda 340, Santiago, Chile. Tel.: +56 2 686 2126; Fax: +56 2 686 2824; E-mail: jlarrain@bio.puc.cl

Received: 19 January 2005; accepted: 14 February 2005; published online: 17 March 2005

Chd, interaction that increased binding of BMP4 to Chd. Bgn was also able to improve the efficiency of Chd–Tsg complexes to block BMP4 activity. Using antisense morpholinos, we demonstrated that Bgn required Chd to induce double axes in *Xenopus*. This work unveiled a new function for Bgn, its ability to regulate BMP4 signaling through modulation of Chd anti-BMP4 activity. We also conclude that Bgn is a novel component of the extracellular machinery that regulates BMP4 signaling during development.

Results

xBgn is expressed during early Xenopus development

In an attempt to study the synthesis of PGs during early development of *Xenopus*, four-cell stage embryos were microinjected with ^{35}S-sulfate, homogenized at stage 9 and then analyzed by gel filtration and SDS–PAGE after treatment with different GAG lyases. The majority of the radioactivity incorporated into PGs was degraded after nitrous acid treatment (Figure 1A, red circles), an indication that they correspond to HSPGs, in agreement with previous reports (Itoh and Sokol, 1994). Interestingly, a small amount of the radioactive PGs was sensitive to chondroitinase ABC (C_{ABC}) treatment (Figure 1A, blue circles). Further analysis by SDS–PAGE showed that blastula stage embryos synthesized a PG that runs with an apparent molecular mass of 200–250 kDa (Figure 1B, brackets). This PG was resistant to heparitinase (Hase) treatment (Figure 1B, lane 2), but sensitive to C_{ABC} (degrades CS and DS chains) and C_{AC} (degrades only CS chains) treatment (Figure 1B, lanes 3 and 4). From these

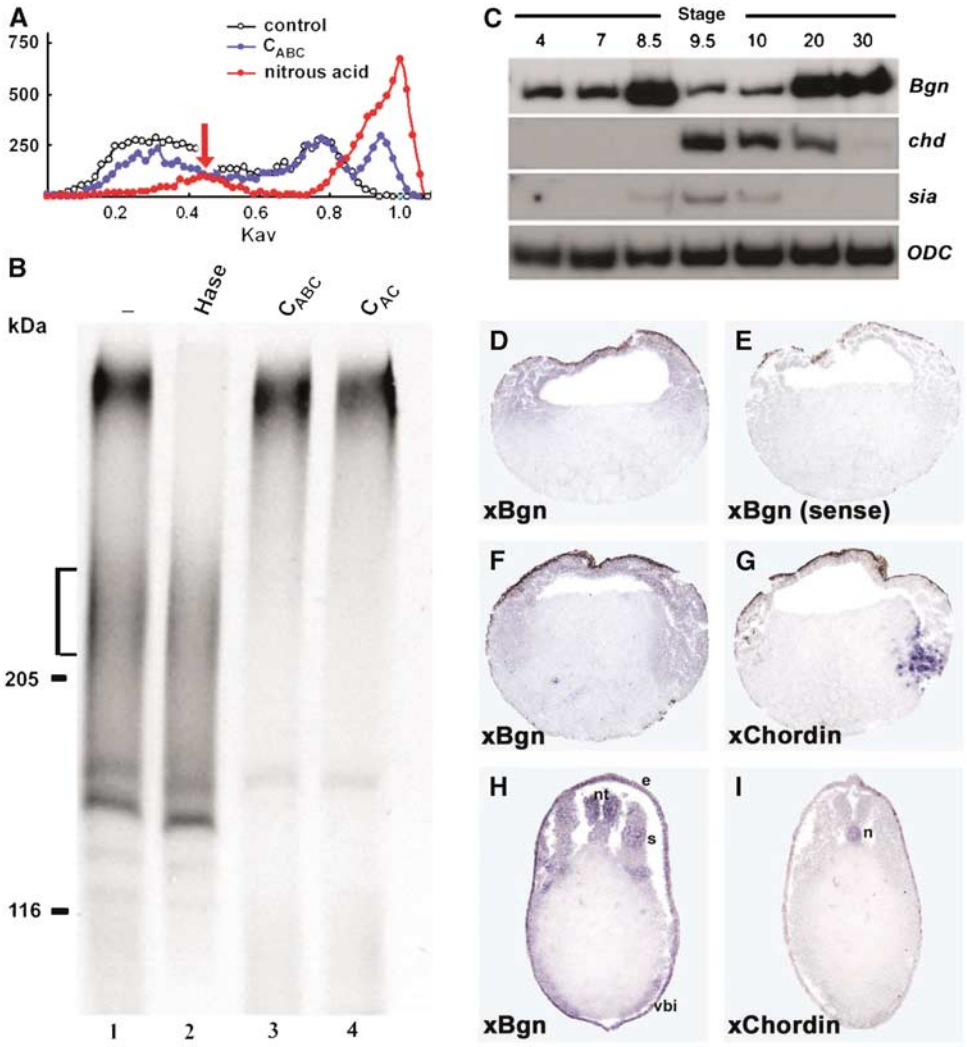

Figure 1 Bgn synthesis and expression during *Xenopus* development. (**A**) Gel filtration profile of ^{35}S-labeled PGs from late blastula stage embryos. Embryos labeled with ^{35}S-sulfate were homogenized at stage 9, homogenates were enriched in PGs by ion exchange chromatography and the labeled extracts were directly loaded in a gel filtration column (white circles) or after treatment with nitrous acid to degrade HS chains (red circles) or after incubation with C_{ABC} to degrade CS and DS chains (blue circles). Note that approximately 5–10% of the radioactivity incorporated into GAGs is resistant to nitrous acid treatment, suggesting that they could correspond to CS/DS PGs (arrow). (**B**) SDS–PAGE analysis of ^{35}S-labeled PGs from late blastula stage embryos. The same samples analyzed above were separated in a 4–15% gradient SDS–PAGE after incubation with Hase (lane 2), C_{ABC} (lane 3) or C_{AC} (lane 4), and then were developed by fluorography. The synthesis of a CSPG with an apparent molecular mass between 200 and 250 kDa is observed (brackets). (**C**) RT–PCR analysis of the expression of *xBgn* at different developmental stages. *chordin* (*chd*) and *siamois* (*sia*) were used as references to detect early zygotic transcription and ODC was used as a loading control. (**D–I**) *xBgn* and *chordin* expression was analyzed by *in situ* hybridization in paraplast sections. Sections of embryos at (D, E) stage 9, (F, G) 10 and (H, I) 28 were analyzed with (D, F, H) *xBgn*, (E) *xBgn* sense or (G, I) *chordin* probes. e: epidermis; n: notochord; nt: neural tube; s: somites; vbi: ventral blood islands.

results, we concluded that blastula stage embryos synthesize HSPGs and a CSPG with a molecular mass between 200 and 250 kDa. When gastrula stage embryos were analyzed, a similar pattern was observed, but the amount of the 200–250 kDa CSPG was lower (data not shown). The molecular mass of the CSPG synthesized at early stages is characteristic of class I members of the SLRP family. This PG family includes Bgn, Dcn and Asporin. They are secreted and abundantly deposited in the extracellular matrix of cartilaginous tissues and play important roles in collagen fibrillogenesis, bone formation, muscle regeneration and TGF-β signaling (Iozzo, 1998; Xu *et al*, 1998; Casar *et al*, 2004). To identify class I members of the SLRP family expressed at gastrula stage, we used a degenerate PCR approach. Using this approach, the only SLRP isolated from gastrula stage embryos was xBgn. RT–PCR and EST database analysis indicated that xBgn is the only member of the SLRP family expressed at this stage (data not shown) and could probably correspond to the CSPG synthesized at gastrula stage. RT–PCR analysis showed that *xBgn* is expressed both maternally and zygotically, with the highest expression levels at stage 8.5 and tail bud stage (Figure 1C). *In situ* hybridization on paraplast sections revealed that at blastula the expression of *xBgn* is high in the ectoderm and declines at gastrula (as expected from the RT–PCR analysis) but could be found in the ectoderm and mesoderm (Figure 1D and F; gastrula sections were developed for longer time). The staining was specific because no signal was detected when the sense probe was used (Figure 1E). Analysis of *xBgn* expression by RT–PCR in explants confirmed that *xBgn* mRNA is preferentially localized to the animal pole at early stages (see Supplementary Figure S1), but no difference between the dorsal and ventral side was observed at stage 10 (data not shown). At tail bud stage, *xBgn* was present in mesodermal and ectodermal derivatives, including somites, neural tube, ventral blood islands, lateral plate and epidermis (Figure 1H). It is important to note that *xBgn* and *chordin* were coexpressed at gastrula stage (Figure 1F and G), and have a complementary expression in the dorsal side at tail bud stage with *chordin* being specifically expressed in the notochord and *Bgn* in somites and neural tube (Figure 1H and I).

Biglycan has dorsalizing activity in Xenopus

The activity of Bgn was studied by microinjection of synthetic mRNA into *Xenopus* embryos. Microinjection of human *Bgn* (*hBgn*) mRNA in four- to eight-cell stage embryos induced secondary axes (Figure 2B), expanded the expression territory of the dorsal marker *MyoD* (Figure 2E) and dorsalized ventral marginal zone (VMZ) explants (Figure 2G). Similar results were obtained when *Xenopus Bgn* (87% homologous at the amino-acid level to hBgn) or mouse *Dcn* were used (data not shown). The phenotypes produced by *hBgn* microinjection were very similar to those produced by the BMP4 antagonist *chordin* (Figure 2C, F and G) and by other secreted anti-BMP4 molecules (Zimmerman *et al*, 1996; Larraín *et al*, 2000; Coffinier *et al*, 2001), raising the possibility that Bgn and Dcn could be a new group of secreted BMP4 antagonists. Analysis of point mutations and deletion constructs of hBgn showed that the CS chains are dispensable for secondary axes-inducing activity and that the active domain resides in the N-terminal domain (see Supplementary Figure S2). BMP4 signaling regulates patterning in *Xenopus* embryos, and the

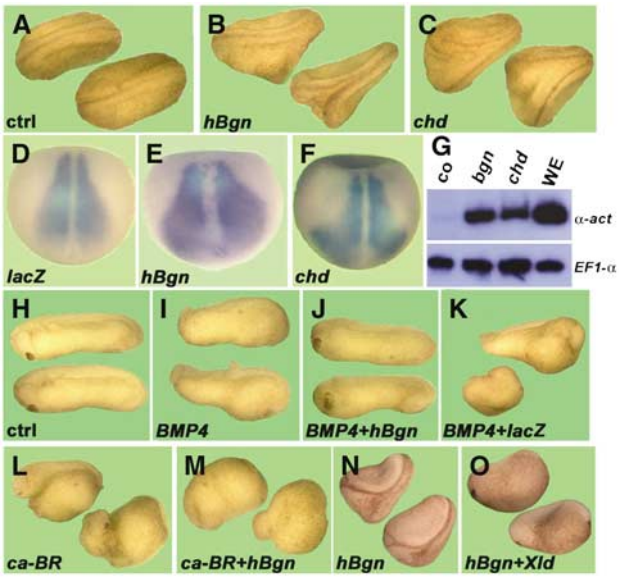

Figure 2 Microinjection of *hBgn* mRNA induces dorsalization and blocks the ventralizing activity of *BMP4* in *Xenopus* embryos. (**A–C**) *hBgn* mRNA induced secondary axes. Embryos at the four- to eight-cell stage were microinjected once in the ventral vegetal side with synthetic mRNA. (B) When 500 pg of *hBgn* was injected, 60% of the embryos had double axis ($N=51$), similar to the results obtained when (C) 5 pg of *chordin* was injected (65%, $N=23$). (**D–F**) *hBgn* mRNA increased the expression of the dorsal marker *MyoD*. Albino embryos were injected four times animally at the four-cell stage with (D) *lacZ* (500 pg/blastomere), (E) *hBgn* (500 pg/blastomere) and (F) *chordin* (75pg/blastomere). The embryos were cultivated until stage 13 and *MyoD* expression was analyzed by *in situ* hybridization. The expansion of the *MyoD* domain of expression after injection of *hBgn* was observed in four out of six embryos. (**G**) *hBgn* dorsalized VMZ explants. Embryos were microinjected twice in the ventral side at the four-cell stage and VMZ was isolated at stage 10 and cultivated until sibling embryos reached stage 26. The expression of the dorsal marker α-*actin* and the loading control *EF-1*α was detected by RT–PCR. Whole embryos were used as an indication of the level of expression in sibling embryos (WE). (**H–M**) *hBgn* blocks the ventralizing activity of BMP4. Embryos were microinjected four times animally with synthetic mRNA for (I) *BMP4*, (J) *BMP4* and *hBgn*, (K) *BMP4* and *lacZ*, (L) *ca-BR* and (M) *ca-BR* and *hBgn*. The number of ventralized embryos (DAI⩽4) for each combination of mRNAs was *BMP4* (10/13), *BMP4/lacZ* (18/21), *BMP4/hBgn* (5/30), *ca-BR* (13/13), *ca-BR/lacZ* (13/14) and *ca-BR/hBgn* (19/21). The total amounts of mRNA used for these experiments were 1.5 ng *hBgn* and *lacZ*, and 250 pg *BMP4* and *ca-BR*. (**N, O**) *Xolloid* inactivates *hBgn*. Embryos at the four- to eight-cell stage were microinjected once in the ventral vegetal side with synthetic mRNA for (N) *hBgn* (63% double axes, $N=53$) and (O) *hBgn* (500 pg) and *Xld* (250 pg, 0%, $N=41$).

ectopic activation of the pathway results in ventralized phenotypes (Fainsod *et al*, 1994). We used this activity as an assay to test the possible anti-BMP4 activity of Bgn. As expected, when four-cell stage embryos were microinjected with *BMP4* synthetic mRNA, ventralized phenotypes were obtained (Figure 2I). These embryos were rescued when *BMP4* was coinjected with *hBgn* mRNA (Figure 2J), but not when *lacZ* mRNA was used (Figure 2K). In contrast, the ventralization induced by a constitutively active BMP4 receptor (*ca-BR*) was not rescued by *hBgn* microinjection (Figure 2L and M), indicating that this CSPG modulates BMP4 signaling in the extracellular space. Interestingly, it has been shown that Bgn is a substrate for the metalloproteinase Tolloid (Scott *et al*, 2000). We have found that

coinjection of *Xolloid* (*Xld*) inactivates *Bgn* (Figure 2N and O), giving further support to the extracellular function of this PG. In summary, we have found that *Bgn* overexpression induces phenotypes characteristic of BMP4 antagonists, counteracts BMP4 activity in *Xenopus* embryos and functions extracellularly.

Biglycan binds BMP4 and modulates its activity

In light of these findings, we decided to study the effect of Bgn on BMP4 signaling at the molecular level. hBgn-flag was obtained from 293T-EBNA cells and purified by anti-flag affinity chromatography (see Supplementary Figure S3). To test whether hBgn-flag can bind BMP4, co-immunoprecipitation assays were performed. hBgn-flag protein was incubated with BMP4, protein complexes immunoprecipitated with anti-flag antibody and the amount of BMP4 precipitated was determined by Western blot. BMP4 was efficiently co-immunoprecipitated with hBgn-flag (Figure 3A, lanes 3 and 4), comparable to the results obtained using recombinant Tsg protein that was previously described as a BMP4-binding protein (Figure 3A, lane 6; Oelgeschläger *et al*, 2000). The interaction between hBgn-flag and BMP4 could be partially competed by a seven-fold excess of BMP2 (Figure 3B, lane 3) but not by FGF, Activin or TGF-β (Figure 3B, lanes 4–6). To determine if the interaction between hBgn and BMP4 is direct, crosslinking experiments were performed. hBgn-flag and BMP4 were incubated, crosslinked and the protein complexes formed analyzed by anti-BMP4 Western blot. In the presence of hBgn-flag, a complex with a molecular mass of approximately 90 kDa was observed (Figure 3C, lane 3). This complex is probably composed of one BMP4 dimer (approximately 35 kDa) and one molecule of hBgn-flag (approximately 50 kDa). The crosslinking of BMP4 to Tsg was used as a positive control (Figure 3C, lane 5). These results indicate that hBgn directly and specifically binds BMP4.

The activity of hBgn-flag protein in BMP4 signaling was tested using two *in vitro* assays: binding of BMP4 to a soluble commercial BMP4 receptor fused to an Fc domain (BR-Fc) and induction of alkaline phosphatase (AP) in C2C12 cells. We found that at low concentrations (1–100 nM), hBgn-flag has no effect on BMP4 activity on any of these assays (data not shown). When an excess of 50-fold or more of hBgn-flag over BMP4 was used, induction of AP and BMP4 binding to the BR-Fc receptor were inhibited (Figure 3D and Supplementary Figure S4). Recent studies using primary cultures of murine calvarie obtained from Bgn null mice indicate that the absence of Bgn reduced the sensitivity of osteoblasts to BMP4 stimulation (Chen *et al*, 2004). As mentioned, a positive effect was not visualized when Bgn protein was added (Figure 3D and data not shown). Because of this, we decided to evaluate the effect of reducing Bgn synthesis using siRNA technology. A mixture of three different siRNA against Bgn was able to specifically reduce the amount of Bgn mRNA compared to wild-type cells or cells

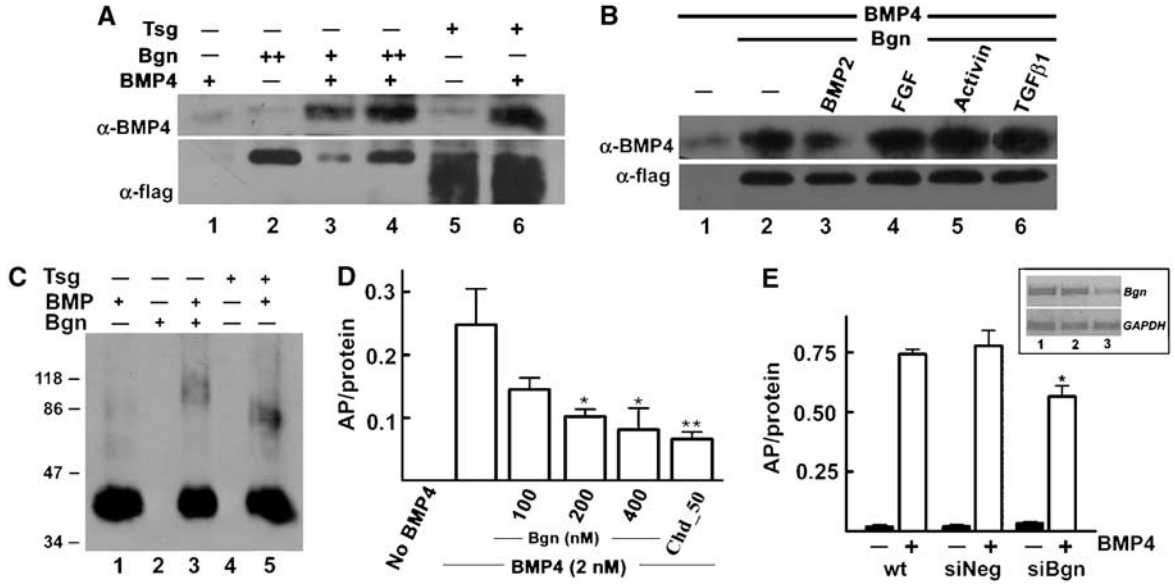

Figure 3 Bgn binds BMP4 directly. (**A**) hBgn-flag binds BMP4. Upper panel: Western blot analysis of BMP4 (10 nM) bound to hBgn-flag (10 and 30 nM, lanes 3 and 4, respectively) after immunoprecipitation of hBgn-flag using anti-flag antibody. As a positive control, 40 nM Tsg-flag was used (lanes 5 and 6). Lower panel: To measure the recovery of hBgn-flag or Tsg after immunoprecipitation, the same membrane was probed with α-flag antibody. (**B**) BMP2 partially competes for the binding of BMP4 to Bgn. Co-immunoprecipitation under the same conditions as in (A) in the presence of a seven-fold excess of BMP2, FGF, Activin or TGF-β1. Note that only BMP2 was able to partially compete for the binding of BMP4 (lane 3). Upper panel: α-BMP4 blot; lower panel: α-flag blot as loading control. (**C**) Bgn directly binds BMP4. hBgn-flag (300 nM) or Tsg (100 nM) was incubated with BMP4 (20 nM), and the complexes formed were covalently crosslinked using disuccinimidyl suberate (DSS) as described (Larraín *et al*, 2000). The samples were separated in a 4–15% gradient gel and developed using α-BMP4 antibody. Note the presence of a band of nearly 90 kDa that could correspond to a complex between a dimer of BMP4 and one molecule of hBgn-flag (lane 3). Tsg and BMP4 formed a complex as expected (lane 5; Oelgeschläger *et al*, 2000). (**D**) High levels of hBgn-flag inhibit alkaline phosphatase (AP) induction by BMP4. AP was measured after 2 days of incubation of C2C12 cells in the presence of 2 nM BMP4. AP induction decreased when increasing amounts of hBgn-flag (100–400 nM) were added. Similar effects were obtained with 50 nM Chd. $*P<0.05$ or $**P<0.01$ compared with AP induction by BMP4 in the absence of any BMP4 antagonist. (**E**) Effect of Bgn siRNA on BMP4 activity. C2C12 cells were transfected with a negative control for siRNA (siNeg) or a mixture of three siRNA for mouse Bgn (siBgn). After 2 days of transfection, cells were incubated with 2 nM BMP4. AP was measured as described above. Inset: Levels of *Bgn* and *GAPDH* mRNA were measured by RT–PCR in wild-type cells (lane 1), and cells transfected with siNeg control (lane 2) or siBgn (lane 3). $*P<0.05$ compared to wild-type or siNeg-treated cells.

treated with an siRNA negative control (Figure 3E, inset). Importantly, the reduction of Bgn synthesis in C2C12 cells produces a decrease of 30% in the ability of BMP4 to induce AP (Figure 3E). These results indicate that in the C2C12 cell assay, Bgn is necessary for BMP4 to attain maximal levels of activity and at high concentrations it could block BMP4 signaling.

Biglycan makes Chordin a better BMP4 antagonist

Our findings in cell culture and biochemical assays do not explain the dorsalizing activity of Bgn in overexpression assays in *Xenopus* embryos. This discrepancy could be explained by the fact that BMP4 signaling in the frog embryo is regulated by a multiprotein complex involving BMP4, Chd and Tsg (Sasai *et al*, 1994; Piccolo *et al*, 1996; Oelgeschläger *et al*, 2000). Chd is one of the key molecules that regulates BMP4 signaling and is highly expressed during early frog development (Sasai *et al*, 1994; Oelgeschläger *et al*, 2003a). We hypothesized that at least some of the Bgn anti-BMP4 activity observed in *Xenopus* assays could depend on the presence of Chd and Tsg. Therefore, we first decided to look into the interaction of Chd and Bgn. Co-immunoprecipitation experiments indicated that Chd did bind to hBgn-flag in solution and this interaction was more easily visualized when the CS chains were enzymatically removed (Figure 4A, lanes 2 and 3). Since *chordin* and *Bgn* are coexpressed in the embryo (Figure 1D–I) and could bind to each other, we analyzed the effect of this interaction on Chd activity. Chd and BMP4 were incubated in the presence of different amounts of hBgn-flag, Chd was pulled down and the amount of BMP4 bound to Chd was measured by Western blot. We found that hBgn-flag increased the binding of BMP4

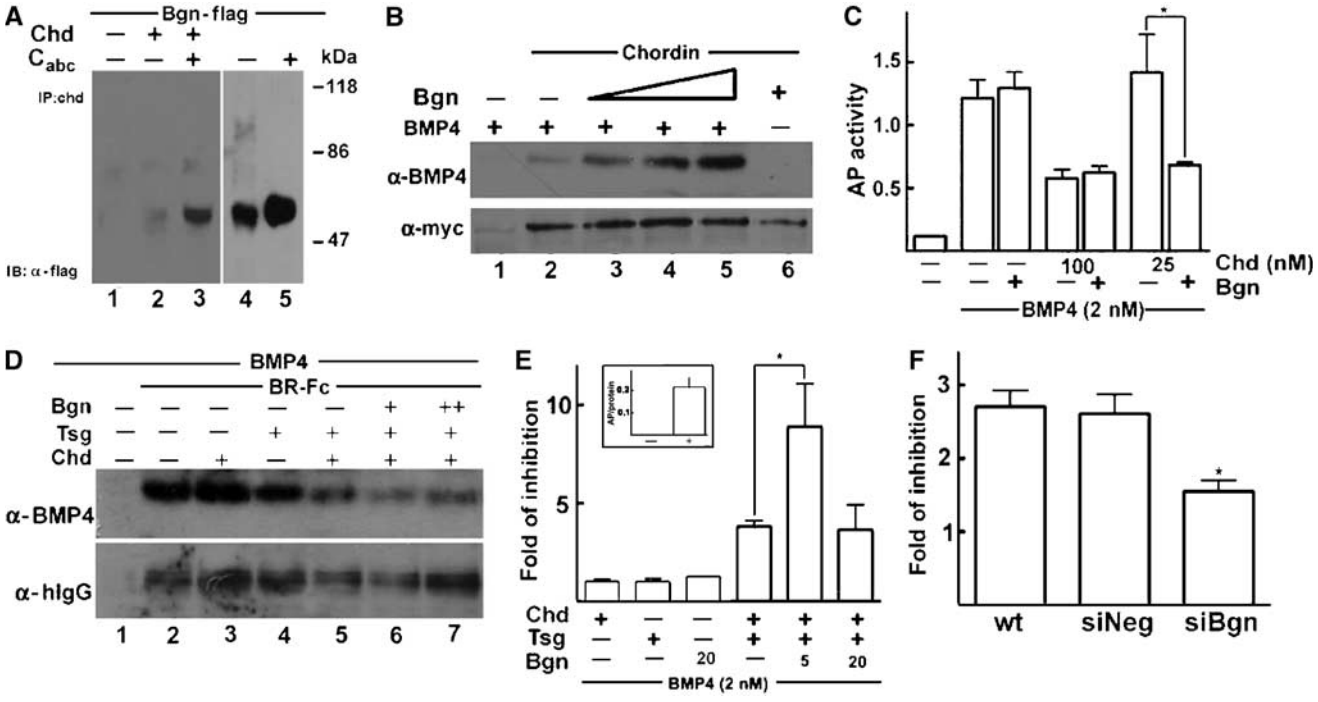

Figure 4 Bgn makes Chd a better BMP4 antagonist. (**A**) Chd interacts with hBgn-flag. Chd-myc and hBgn-flag were incubated and pulled down using α-Nchd antibody. The amount of hBgn-flag precipitated was visualized by α-flag Western blot. The hBgn-flag used was not treated (lane 2) or treated (lane 3) with C_{ABC}. For reference, hBgn inputs untreated and treated with C_{ABC} were loaded (lanes 4 and 5, respectively). Note that Chd precipitates the Bgn core protein from untreated and treated inputs, and the difference in the efficiency of the interaction could be explained by the higher amounts of Bgn core protein present in the inputs when the samples were treated with C_{ABC} (compare lanes 4 and 5). (**B**) Chd binds BMP4 more efficiently in the presence of hBgn-flag. Upper panel: Chd baculovirus protein was incubated with BMP4 (10 nM) in the presence of hBgn (5, 10 and 20 nM), and the amount of BMP4 bound to Chd was determined by immunoprecipitation with α-Nchd followed by α-BMP4 immunoblot. Lower panel: The amount of Chd precipitated is revealed by α-myc Western blot. (**C**) Bgn increases Chd anti-BMP4 activity in C2C12 cells. AP induction assay was performed as in Figure 3D. In this case, the effect of 25 nM hBgn-flag in the presence of different Chd concentrations was tested. At suboptimal concentrations of Chd (25 nM), Bgn cooperated with Chd in blocking BMP4 activity. $^*P<0.05$ when the effect of Bgn and Chd (25 nM) was compared to the effect of Chd (25 nM) alone. (**D**) hBgn-flag increases the ability of Chd and Tsg to compete for BMP4 binding to a soluble receptor. BMP4 (2 nM) was incubated with 10 nM BR-Fc (lane 2) in the presence of 10 nM Chd (lane 3), 10 nM Tsg (lane 4), Chd and Tsg (lane 5), and Chd/Tsg plus 2.5 nM (lane 6) or 5.0 nM hBgn-flag (lane 7). The receptor was precipitated with protein-A-agarose and the amount of BMP4 bound was determined by α-BMP4 Western blot (upper panel). Western blot using α-human IgG against BR-Fc was performed as loading control (lower panel). (**E**) hBgn-flag increases the anti-BMP4 activity of Chd/Tsg complexes in C2C12 cells. The ability of Chd, Tsg and Bgn proteins to inhibit BMP4 activity was tested in C2C12 cells. The graphic shows the fold of inhibition obtained by each protein alone or a mixture of them. Fold of inhibition indicates the times that each protein decreases the induction of AP by 2 nM BMP4 alone. The maximal level of induction obtained by BMP4 alone (inset) was used as reference to calculate the fold of inhibition. It was shown that 10 nM Chd, 20 nM Tsg and 20 nM hBgn have no effect when added separately. Chd and Tsg together inhibit AP induction 3.8-fold as expected from their known cooperative effect. When hBgn (5 nM) was added, an even stronger inhibition was observed (8.9 times inhibition). When higher amounts of hBgn were used (20 nM), the effect of Bgn on Chd/Tsg complexes was lost. $^*P<0.05$ when the effect of Chd/Tsg/Bgn was compared to the effect of Chd/Tsg. (**F**) Bgn siRNA reduces the inhibition of BMP4 by Chd/Tsg complexes. Wild-type C2C12 cells or cells treated with siNeg or siBgn were induced with BMP4 in the absence or presence of 5 nM Chd and 10 nM Tsg. After 2 days, the levels of AP were measured. Note that 5 nM Chd and 10 nM Tsg protein inhibit BMP4 activity approximately 2.7 times (wild-type and siNeg cells) and this effect is reduced approximately 1.54 times in cells treated with siBgn. $^*P<0.05$ when siBgn effect is compared to wild-type and siNeg cells.

to Chd in a concentration-dependent manner (Figure 4B, lanes 2–5). To determine if the increased binding of BMP4 to Chd in the presence of hBgn-flag results in a more potent anti-BMP4 activity, we took advantage of the AP induction assay in C2C12 cells. At high concentrations of Chd (100 nM), the presence of 20 nM hBgn-flag had no effect on its inhibitory activity. However, when suboptimal amounts of Chd (25 nM) were used, the presence of 20 nM hBgn-flag potentiated the inhibition of AP induction (Figure 4C).

As mentioned above, Tsg is another extracellular protein that regulates BMP4 signaling in *Xenopus* embryos. Tsg is a secreted protein that binds BMP4 and has dual activities on BMP4 signaling: it cooperates in BMP antagonism by increasing binding of BMP4 to Chd, and promotes BMP4 signaling when Tolloid cleaves Chd (Oelgeschläger *et al*, 2000; Larraín *et al*, 2001; Scott *et al*, 2001). Then, we decided to study the effect of Bgn on Chd–Tsg anti-BMP4 activity. First, we tested the effect of hBgn-flag on the ability of Chd and Tsg to compete for the binding of BMP4 to soluble BR-Fc. Chd and Tsg (10 nM) have no effect when added separately (Figure 4D, lanes 3 and 4, respectively); however, when added together, they compete for the binding of BMP4 to the receptor (Figure 4D, lane 5), reflecting the already described cooperative effect between these two molecules (Oelgeschläger *et al*, 2000; Larraín *et al*, 2001). Importantly, when 2.5 and 5 nM hBgn-flag was included, BMP4 binding to the receptor was even more efficiently competed (Figure 4D, lane 6). A similar experiment was performed using the AP induction assay in C2C12 cells. Chd (10 nM) and Tsg (20 nM) have no effects on BMP4 activity when added separately (Figure 4E). As expected, addition of Chd and Tsg together showed a strong cooperative effect (Oelgeschläger *et al*, 2000; Larraín *et al*, 2001), and AP induction was inhibited 3.8 times (Figure 4E). When 5 nM hBgn-flag was included with Chd and Tsg, the extent of inhibition of BMP4 activity raised 8.9 times, indicating that Bgn makes the Chd/Tsg complex an even better BMP4 antagonist (Figure 4E). It is interesting to note that the cooperative effect on BMP4 signaling required a precise stoichiometry between the three molecules, since in the presence of higher amounts of hBgn-flag, the cooperative effect was lost (Figure 4D, lane 7, and Figure 4E). To further test the function of Bgn, we evaluated the effect of decreasing the levels of Bgn on the activity of Chd/Tsg complexes. We found that Chd/Tsg complexes are less efficient in the inhibition of BMP4 when the endogenous levels of Bgn were reduced by siRNA (Figure 4F). In summary, we conclude that Bgn binds Chd and makes it a better BMP4-binding protein enhancing its anti-BMP4 activity.

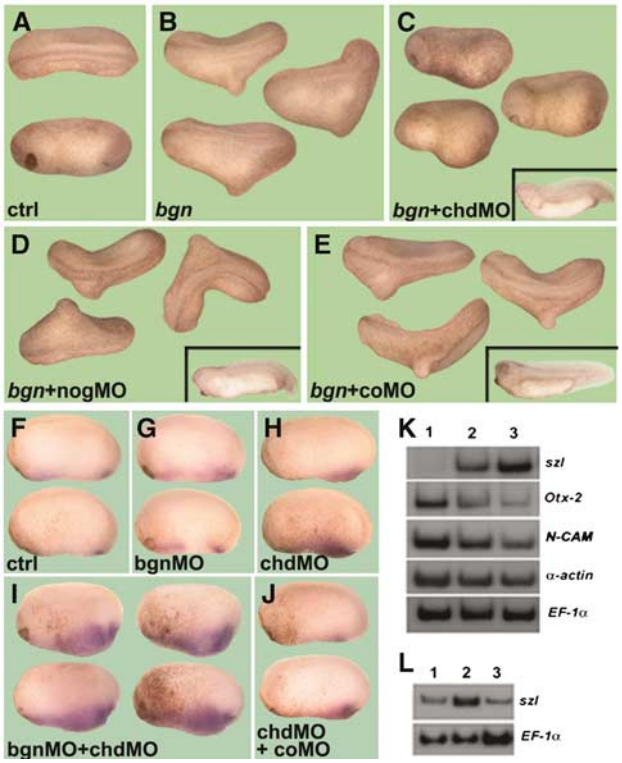

Figure 5 *hBgn* requires Chd to induce double axes in *Xenopus* embryos. (**A–E**) Secondary axes induced by *hBgn* require Chd. Embryos were injected at the four-cell stage into the B-tier of each dorsal blastomere with 8 ng of (C) chdMO (Oelgeschläger *et al*, 2003a), (D) nogMO (Kuroda *et al*, 2004) or (E) coMO followed by one ventral microinjection in the vegetal side of *hBgn* (500 pg) synthetic mRNA. The number of double axes induced by each combination of mRNA and morpholinos was *bgn* (44/77), *bgn* + chdMO (0/68), *bgn* + nogMO (36/80) and *bgn* + coMO (34/53). The insets in panels C–E show the phenotypes obtained by microinjection of the different morpholinos. (**F–J**) bgnMO and chdMO cooperate in the ventralization of *Xenopus* embryos. Embryos were injected four times animally at the four-cell stage with (G) bgnMO (8 ng/blastomere), (H) chdMO (1.0 ng/blastomere), (I) chdMO + bgnMO and (J) chdMO + coMO. Development was stopped at stage 20 and *in situ* hybridization for *sizzled* was performed. Eight out of 13 embryos showed an expanded domain of *szl* expression after microinjection of chdMO and bgnMO together. None of the embryos injected with each morpholino alone or with chdMO and coMO have an expansion of the *szl* domain ($N = 7–11$). (**K**) Control embryos (lane 1), injected with chdMO (lane 2) or with chdMO and bgnMO (lane 3) were cultured up to stage 25 and analyzed by RT–PCR for different molecular markers. (**L**) RT–PCR analysis of *szl* to show rescue of the effect of bgnMO. Embryos were injected with chdMO (lane 1), chdMO and bgnMO (lane 2) and chdMO, bgnMO and *hBgn* synthetic mRNA (lane 3).

Biglycan functions as a cofactor of Chordin in Xenopus embryos

The results obtained in cell culture and biochemical assays raised the possibility that the dorsalizing activity of *hBgn* in *Xenopus* embryos could be explained by its ability to increase Chd anti-BMP4 activity. To study this, we took advantage of the recently described antisense Chd morpholinos (chdMO) that knock down the synthesis of Chd in *Xenopus* embryos (Oelgeschläger *et al*, 2003a). *hBgn* was unable to induce the formation of double axes in embryos that were microinjected with chdMO (Figure 5B and C). Contrary to this, when noggin morpholinos (nogMO; Kuroda *et al*, 2004) or control morpholinos (coMO) were used, *hBgn* mRNA retained its ability to induce double axes (Figure 5D and E), indicating that the dorsalizing activity of Bgn depends specifically on Chd but not on other BMP4 antagonists (Zimmerman *et al*, 1996). These results demonstrate that Bgn requires Chd in order to induce secondary axes in *Xenopus* embryos and support the hypothesis that Bgn acts as a Chd cofactor *in vivo*.

The *in vivo* relevance of Bgn was tested using morpholinos. We have found that a mixture of two morpholinos against two pseudoalleles of Bgn (bgnMO; see Supplementary Figure S5) has no evident phenotype (data not shown). To further analyze the cooperativity of Chd and Bgn in *Xenopus* embryos, we studied the effect of coinjection of bgnMO with suboptimal amounts of chdMO. As a measure

Table I Cooperativity between chdMO and bgnMO

	%[a]
Wild type	0 (35)
coMO	0 (32)
bgnMO	0 (15)
chdMO	28 (59)
chdMO;coMO	20 (21)
chdMO;bgnMO	69 (49)
chdMO;bgnMO + *Chd* 2.0 pg	16 (31)

[a]Embryos with ventralized phenotype or with a broader domain of expression for *sizzled*. Numbers in parentheses indicate the total amount of embryos analyzed for each point.

of the levels of Chd activity, we evaluated the expression of *sizzled* (*szl*) by *in situ* hybridization. This ventral marker is highly expanded when embryos are completely depleted of Chd protein (Oelgeschläger *et al*, 2003a). Embryos injected with suboptimal amounts of chdMO or bgnMO have normal levels of *szl* (Figure 5F–H). When both morpholinos were injected together, an increase in the *szl*-positive domain was observed (Figure 5I). This effect was not observed when coMO was coinjected with chdMO (Figure 5J). Importantly, this effect could be rescued by coinjection of *chordin* mRNA (Table I), indicating that it is specific. To further analyze the cooperative effect between chdMO and bgnMO, we evaluated the level of expression of different markers by RT–PCR of whole embryos. Embryos injected with suboptimal amounts of chdMO have a small increase in the levels of the ventral marker *szl* and a decrease in the neural marker *N-CAM* and in the anterior marker *Otx-2* (Figure 5K, compare lanes 1 and 2). When bgnMO was coinjected with chdMO, the levels of *szl* were increased whereas *N-CAM* and *Otx-2* expression was decreased with respect to the embryos injected with chdMO alone (Figure 5K, compare lanes 2 and 3). The fact that the increased expression of *szl* in embryos coinjected with chdMO and bgnMO could be rescued by *hBgn* mRNA indicates that the effect of the morpholinos is specific (Figure 5L). Together, these experiments showed that Bgn is a cofactor of Chd that modulates BMP4 signaling by making Chd a better BMP4 antagonist.

Discussion

The regulation of BMP4 signaling in the extracellular space by a network of secreted proteins, which include Chd, Tsg and the metalloproteinase Tolloid, is a paradigm for understanding extracellular cell–cell signaling. Here, we have introduced Bgn as a new component of this extracellular network. We have shown, using biochemical assays, that Bgn binds BMP4 and Chd and makes Chd a more efficient binder of BMP4. In cell culture assays, Bgn increases the ability of Chd/Tsg complexes to inhibit BMP4, and when Bgn levels are decreased using siRNA, the anti-BMP4 activity of these complexes is reduced. Experiments in *Xenopus* embryos showed that induction of secondary axes by *Bgn* requires Chd and that Bgn cooperates with Chd. Experiments using bgnMO have failed to show any phenotype, a result that could be explained by the high levels of maternal Bgn or because of redundancy with Tsukushi, a recently identified member of the SLRP class IV family that is expressed early in frog and chick embryos and also functions as a BMP4 antagonist (Ohta *et al*, 2004). We concluded from all these results that Bgn is a Chd cofactor that regulates BMP4 signaling through modulation of Chd anti-BMP4 activity. Our results using siRNA in C2C12 cells and the analysis of Bgn null osteoblasts (Chen *et al*, 2004) indicate that Bgn could also have a positive effect on BMP4; so far we have no evidence for such a function during *Xenopus* development. Evidences for these two opposing activities of Bgn have been observed in Bgn null mice. In these animals, bone is undermineralized while tendons undergo ectopic calcification, suggesting both stimulating and inhibiting functions for Bgn (Ameye and Young, 2002; Ameye *et al*, 2002). Furthermore, analysis of Bgn/Dcn null mice indicates increased growth factor action in osteogenic stem cells (M Young, personal communication).

We speculate that Bgn will be one more step in the extracellular regulation of BMP4 activity by Chd; its presence could modulate the interaction between Chd and Tsg and also interaction with Tolloid. It is already known that the presence of Tsg in the Chd/BMP4 complex produces a variety of effects on BMP4 signaling; it antagonizes BMP4 activity in the presence of intact Chd by making a ternary complex, and promotes signaling after Tolloid cleavage (Oelgeschläger *et al*, 2000; Larraín *et al*, 2001; Scott *et al*, 2001). Furthermore, Tsg stimulates the proteolytic cleavage of Chd by Tolloid and might also influence the preference of Tolloid for specific cleavage sites in Chd, producing different Chd fragments that could have novel activities (Yu *et al*, 2000; Shimmi and O'Connor, 2003). Interestingly, it has been reported that Bgn is secreted as pro-Bgn and is processed by Tolloid (Scott *et al*, 2000), and here we showed that Bgn function is regulated by Xld. Further studies will have to address the potential functional relationship of Bgn with Tsg and Tolloid, in particular if the Chd–Bgn interaction affects Tsg binding and/or Tolloid cleavage of Chd. It has been previously reported that Dcn and Bgn can bind TGF-β (Iozzo, 1998), but according to our results this growth factor does not compete for the binding of BMP4 to hBgn (Figure 3B, lane 6), suggesting that they could bind to independent sites or with different affinities. To answer this, we prepared an hBgn construct with the potential TGF-β-binding domain removed (Schonherr *et al*, 1998) and tested its activity in *Xenopus* embryos. This construct retains the double axes-inducing activity, suggesting that BMP4 and TGF-β could bind to different domains in hBgn and that the dorsalizing activity of Bgn does not involve the TGF-β-binding domain (see Supplementary Figure S3). Chd is one of the main players in the establishment of dorsoventral patterning in vertebrate as well in invertebrate embryos. The early expression pattern of xBgn, the role of Bgn as a Chd cofactor and the finding that bgnMO enhanced the ventralized phenotype obtained using suboptimal amounts of chdMO suggest that Bgn could regulate early dorsoventral patterning. The possibility that Bgn could also have an effect on BMP4, in the absence of Chd, especially considering its high expression in the animal cap at blastula stage needs to be addressed. Finally, mice lacking functional Bgn develop an osteoporosis-like phenotype (Xu *et al*, 1998) and BMPs have been classically involved in bone metabolism. Our findings of a functional interaction between Bgn and BMP4 could be an important contribution not only to answer questions related to early development, but also for the understanding of bone biology.

Materials and methods

Embryos and explants

In vitro fertilizations, embryo culture, microinjections, explants culture and *in situ* hybridizations on paraplast sections were performed as described (Lemaire and Gurdon, 1994; Sive *et al*, 2000). All mRNAs were synthesized *in vitro* with SP6 or T7 polymerase using the Message Machine kit (Ambion Inc.).

Proteoglycan analysis

Embryos were microinjected with 0.1 μCi of $^{35}S\text{-}SO_4^{2-}$ into each blastomere at the two- to four-cell stage and developed until blastula or gastrula stage. Embryos were homogenized in 10 mM Tris pH 7.5, 150 mM NaCl and 0.5% Triton X-100 and PGs were concentrated by ion exchange chromatography and then analyzed by gel filtration and SDS–PAGE as described (Riquelme *et al*, 2001).

RT–PCR and morpholino oligonucleotides

RT–PCR assays were performed in the exponential phase of amplification and with primers as described (Larraín *et al*, 2001). xBgn primers used were Fw 5′-GGTTATAGTCAACAACAAGA-3′ and Rv 5′-CAATGCCTCCATTTTCCAGA-3′ and the PCR amplification was 94°C for 1 min, 50°C for 1 min and 72°C for 1 min (30 cycles). chdMO 1 and 2 were used as described (Oelgeschläger *et al*, 2003a). bgnMO were xBgn-Mo1: 5′-AGCATAAGAGAAGCAATACCTTCAT-3′ and xBgn-Mo2: 5′-CAATATACAAAGGTTCCTTCCAGGC-3′. A 1:1 mixture of both morpholinos was used in our experiments (bgnMO; see Supplementary Figure S5).

Constructs

To identify SLRP expressed at early embryonic stages, a degenerate PCR approach was used. Gastrula stage cDNA was amplified using the following primers: Fw 5′-GTIGTICAITGCTCIGATYTIGGT-3′ and Rv 5′-AGITTGTTGTTITYIAAGTGIAGITCICT-3′. The PCR conditions were 96°C for 45 s, 58°C for 4 min and 72°C for 3 min (45 cycles) as described (Buck and Axel, 1991). The product was ligated into pGEM-T Easy vector (Promega) and five clones were sequenced (all of them were xBgn). Full-length xBgn was obtained by PCR using Fw 5′-ATGAAGGTATTGCTTCTCTTATGC-3′ and Rv 5′-TTACTTCCTG TAATTGCCAAACTG-3′ designed from the full-length xBgn nucleotide sequence available in the Genebank database (AB037269). xBgn was subsequently subcloned into pCS2+ and pcDNA3.1+ expression vectors. We found that the mRNA prepared from pcDNA3.1+ was the more active and was used for all experiments. Epitope tag full-length hBgn was obtained by PCR using the primers Fw 5′-GGTCCAGAATTCATGTGGCCCCTGTGG-3′ and Rv 5′-CTCGAG TTACTTGTCATCGTCGTCCTTGTAGTCCTTTTTGTAGTTGCCAAAC-3′ and the product was subcloned in the expression vector pCEP4.

Immunoprecipitation, crosslinking and C2C12 cell culture assays

HEK293-EBNA cells were transfected with pCEP:hBgn-flag to prepare a stable line. Recombinant hBgn-flag was obtained from the conditioned medium, treated with C_{ABC} and purified by anti-flag affinity chromatography as described (Oelgeschläger *et al*, 2003b). Immunoprecipitations and crosslinking assays were performed as described (Larraín *et al*, 2000). AP induction in C2C12 cells by BMP4 was measured as described (Nakayama *et al*, 2004). BMP4, Chd, Tsg and BMPRIb-Fc were obtained from R&D systems and used for most of the experiments, except for co-immunoprecipitations and crosslinking shown in Figure 4A and B and Supplementary Figure S4 where Chd-myc from baculovirus was used (Piccolo *et al*, 1996). Statistical analysis was performed using the software GraphPad Prism applying ANOVA analysis.

siRNA knockdown of Bgn in C2C12 cells

At day 1, 70 000 cells/well were plated in a six-well plate. At day 2, they were transfected using siPORT™ Lipid (Ambion®) containing 250 nM mouse Bgn siRNA (siBgn) in Opti-MEM FBS free. At day 3, the cells were trypsinized and 27 000 cells/well were plated in a 96-well plate. At 1 day after plating, cells were induced with BMP4, and AP activity was measured 2 days later. Cells were also harvested to prepare total RNA for RT–PCR analysis. siBgn corresponds to a mixture of three RNA duplexes that base-pair to Bgn gene in three different positions (64, 508 and 955). The sequences are siBgn64 5′-GGGUUUCUGGGACUUCACCUU-3′, siBgn508 5′-CCGUAUCCGCA AAGUGCCCUU-3′ and siBgn955 5′-UGACUUCUGUCCUAUGGGCU U-3′. Bgn PCR analysis was performed using the primers Fw 5′-TCC CCAGGAACATTGACCAT-3′ and Rv 5′-GTTCAAAGCCACTGTTCTCCA-3′, which amplify a 625 bp fragment. Amplification conditions were 94°C for 1 min, 55°C for 1 min and 72°C for 1 min (25 cycles) using as template 2% of cDNA reaction and GAPDH as loading control.

Supplementary data

Supplementary data are available at *The EMBO Journal* Online.

Acknowledgements

We thank G Olivares, F Faunes, O Wessely, M Oelgeschläger and M Concha for comments on the manuscript, G Olivares and F Faunes for their help in the statistical analysis and JP Guzmán for technical assistance. MM and ML are PhD fellows from CONICYT. EB is an HHMI International Scholar. This work was supported by FONDECYT 1030481, Fundación Andes C-13760, MIFAB and TWAS02-501.

References

Ameye L, Aria D, Jepsen K, Oldberg A, Xu T, Young MF (2002) Abnormal collagen fibrils in tendons of biglycan/fibromodulin-deficient mice lead to gait impairment, ectopic ossification, and osteoarthritis. *FASEB J* **16:** 673–680

Ameye L, Young MF (2002) Mice deficient in small leucine-rich proteoglycans: novel *in vivo* models for osteoporosis, osteoarthritis, Ehlers–Danlos syndrome, muscular dystrophy, and corneal diseases. *Glycobiology* **12:** 107R–116R

Bernfield M, Gotte M, Park PW, Reizes O, Fitzgerald ML, Lincecum J, Zako M (1999) Functions of cell surface heparan sulfate proteoglycans. *Annu Rev Biochem* **68:** 729–777

Buck L, Axel R (1991) A novel multigene family may encode odorant receptors: a molecular basis for odor recognition. *Cell* **65:** 175–187

Casar JC, McKechnie BA, Fallon JR, Young MF, Brandan E (2004) Transient up-regulation of biglycan during skeletal muscle regeneration: delayed fiber growth along with decorin increase in biglycan-deficient mice. *Dev Biol* **268:** 358–371

Chen XD, Fisher LW, Gehron P, Young M (2004) The small leucine-rich proteoglycan biglycan modulates BMP-4-induced osteoblast differentiation. *FASEB J* **18:** 948–958

Coffinier C, Tran U, Larraín J, De Robertis EM (2001) Neuralin-1 is a novel Chordin-related molecule expressed in the mouse neural plate. *Mech Dev* **100:** 119–122

De Robertis EM, Larraín J, Oelgeschläger M, Wessely O (2000) The establishment of Spemann's Organizer and patterning of the vertebrate embryo. *Nat Rev Genet* **1:** 171–181

Fainsod A, Steinbeisser H, De Robertis EM (1994) On the function of BMP4 in patterning the marginal zone of the *Xenopus* embryo. *EMBO J* **13:** 5015–5025

Freeman M, Gurdon JB (2002) Regulatory principles of developmental signalling. *Annu Rev Cell Biol* **18:** 515–539

Iozzo RV (1998) Matrix proteoglycans: from molecular design to cellular function. *Annu Rev Biochem* **67:** 609–652

Itoh K, Sokol SY (1994) Heparan sulphate proteoglycans are required for mesoderm formation in *Xenopus* embryos. *Development* **120:** 2703–2711

Kuroda H, Wessely O, Robertis EM (2004) Neural Induction in *Xenopus*: requirement for ectodermal and endomesodermal signals via chordin, noggin, beta-catenin, and cerberus. *PLoS Biol* **5:** 0623–0634

Larraín J, Bachiller D, Lu B, Agius E, Piccolo S, De Robertis EM (2000) BMP4-binding modules in chordin: a model for signalling regulation in the extracellular space. *Development* **127:** 821–830

Larraín J, Oelgeschlager M, Ketpura NI, Reversade B, Zakin L, De Robertis EM (2001) Proteolytic cleavage of Chordin as a switch

for the dual activities of Twisted gastrulation on BMP4. *Development* **128:** 4439–4447

Lemaire P, Gurdon J (1994) A role for cytoplasmic determinants in mesoderm patterning: cell-autonomous activation of the goosecoid and Xwnt-8 genes along the dorsoventral axis of early *Xenopus* embryos. *Development* **120:** 1191–1199

Nakayama N, Han CY, Cam L, Lee JI, Pretorius J, Fisher S, Rosenfeld R, Scully S, Nishinakamura R, Duryea D, Van G, Bolon B, Yokota T, Zhang K (2004) A novel chordin-like BMP4 inhibitor, CHL2, expressed preferentially in chondrocytes of developing cartilage and osteoarthritic joint cartilage. *Development* **131:** 229–240

Oelgeschläger M, Kuroda H, Reversade B, De Robertis EM (2003a) Chordin is required for the Spemann organizer transplantation phenomenon in *Xenopus* embryos. *Dev Cell* **4:** 219–230

Oelgeschläger M, Larraín J, Geissert D, De Robertis EM (2000) The evolutionarily conserved BMP4-binding protein Twisted gastrulation promotes BMP4 signalling. *Nature* **405:** 757–763

Oelgeschläger M, Reversade B, Larrain J, Little S, Mullins MC, De Robertis EM (2003b) The pro-BMP4 activity of Twisted gastrulation is independent of BMP4 binding. *Development* **130:** 4047–4056

Ohta K, Lupo G, Kuriyama S, Keynes R, Holt CE, Harris WA, Tanaka H, Ohnuma S (2004) Tsukushi functions as an organizer inducer by inhibition of BMP activity in cooperation with chordin. *Dev Cell* **7:** 347–358

Perrimon N, Bernfield M (2000) Specificities of heparan sulphate proteoglycans in developmental processes. *Nature* **404:** 725–728

Piccolo S, Sasai Y, Lu B, De Robertis EM (1996) Dorsoventral patterning in *Xenopus*: inhibition of ventral signals by direct binding of Chordin to BMP4. *Cell* **86:** 589–598

Riquelme C, Larrain J, Schonherr E, Henriquez JP, Kresse H, Brandan E (2001) Antisense inhibition of decorin expression in myoblasts decreases cell responsiveness to transforming growth factor beta and accelerates skeletal muscle differentiation. *J Biol Chem* **276:** 3589–3596

Sasai Y, Lu B, Steinbeisse H, Geissert D, Gont LK, De Robertis EM (1994) *Xenopus* chordin: a novel dorsalizing factor activated by organizer-specific homeobox genes. *Cell* **79:** 779–790

Schonherr E, Broszat M, Brandan E, Bruckner P, Kresse H (1998) Decorin core protein fragment Leu155-Val260 interacts with TGF-beta but does not compete for decorin binding to type I collagen. *Arch Biochem Biophys* **355:** 241–248

Scott IC, Blitz IL, Pappano WN, Maas SA, Cho KW, Greenspan DS (2001) Homologues of Twisted gastrulation are extracellular co-factors in antagonism of BMP signalling. *Nature* **410:** 475–478

Scott IC, Imamura Y, Pappano WN, Troedel JM, Recklies AD, Roughley PJ, Greenspan DS (2000) Bone morphogenetic protein-1 processes probiglycan. *J Biol Chem* **275:** 30504–30511

Shimmi O, O'Connor MB (2003) Physical properties of Tld, Sog, Tsg and Dpp protein interactions are predicted to help create a sharp boundary in Bmp signals during dorsoventral patterning of the *Drosophila* embryo. *Development* **130:** 4673–4682

Sive HL, Grainger RM, Harland RM (2000) *Early Development of Xenopus laevis: A Laboratory Manual*. Cold Spring Harbor, NY: Cold Spring Harbor Laboratory Press

Xu T, Bianco P, Fisher LW, Longenecker G, Smith E, Goldstein S, Bonadio J, Boskey A, Heegaard AM, Sommer B, Satomura K, Dominguez P, Zhao C, Kulkarni AB, Robey PG, Young MF (1998) Targeted disruption of the Biglycan gene leads to an osteoporosis-like phenotype in mice. *Nat Genet* **20:** 78–82

Yu K, Srinivasan S, Shimmi O, Biehs B, Rashka KE, Kimelman D, O'Connor MB, Bier E (2000) Processing of the *Drosophila* Sog protein creates a novel BMP inhibitory activity. *Development* **127:** 2143–2154

Zimmerman LB, De Jesús-Escobar JM, Harland RM (1996) The Spemann organizer signal noggin binds and inactivates bone morphogenetic protein 4. *Cell* **86:** 599–606